

Rothamsted Repository Download

A - Papers appearing in refereed journals

Reynolds, A. M. 2019. On the origin of the tensile strength of insect swarms. *Physical Biology*.

The publisher's version can be accessed at:

- <https://dx.doi.org/10.1088/1478-3975/ab12b9>
- <http://iopscience.iop.org/10.1088/1478-3975/ab12b9>

The output can be accessed at: <https://repository.rothamsted.ac.uk/item/8wq5q>.

© 26 March 2019, Rothamsted Research. Licensed under the Creative Commons CC BY.

On the origin of the tensile strength of insect swarms

Andy M. Reynolds

Rothamsted Research, Harpenden, Hertfordshire, AL5 2JQ, UK

5

Abstract Traditionally animal groups have been characterized by the macroscopic patterns that they form. It is now recognised that such patterns convey limited information about the nature of the aggregation as a whole. Aggregate properties cannot be determined by passive observations alone; instead one must interact with them. One of the first such dynamical tests revealed that swarms of flying insects have macroscopic mechanical properties similar to solids, including a finite Young's modulus and yield strength. Here I show, somewhat counterintuitively, that the emergence of these solid-like properties can be attributed to centre-of-mass movements (heat). This suggests that perturbations can drive phase transitions.

15 Tel: +44 (0)1582 763133

Fax: +44 (0)1582 760981

Email: andy.reynolds@rothamsted.ac.uk

PACS 87.23.Ge - Dynamics of social systems

20 PACS 05.10.Gg – Stochastic analysis methods (Fokker-Planck, Langevin etc.)

Introduction

25 Sparse swarms of flying insects show a high degree of spatial cohesion and are a form of collective animal behaviour; albeit one different from flocks and schools as they do not display ordered collective movements [Okubo 1986, Kelley and Ouellette 2013, Puckett et al. 2014]. Instead each individual insect moves erratically and seemingly at random within the swarm. The occurrence of these swarms makes it clear that group order and morphology are not sufficient to accurately describe animal aggregations. Indeed, it is now recognized that the
30 properties of animal aggregates cannot be determined by passive observation alone; instead one must interact with them, by for example applying controlled perturbations [Ouellette 2017]. This approach allows for the extraction of emergent group properties that are not directly linked to the characteristics of the individuals. Ni and Ouellette [2016] were the first to examine swarms of flying insects (the non-biting midge *Chironomus riparius*) in this way and did so by
35 placing them under an effective load, i.e., by manipulating ground-based visual features, so-called ‘swarm markers’, over which swarms form. Ni and Ouellette [2016] showed that a swarm can be quasi-statically pulled apart into multiple daughter swarms which were centred over each marker once the marker separation was large enough. For intermediate separations the daughter swarms were pulled away from the centres of their respective markers and into
40 a stable ‘neck’ region that linked them. This indicates that the swarms have mechanical properties similar to solids, including a finite Young’s modulus and yield strength, and it shows that they lack a viscous flow regime.

Here I show how these emergent mechanical properties of insect swarms can
45 be deduced from the simple, analytically-tractable model of Reynolds et al. [2017] which is in close accord with a plethora of other (albeit passive) observations of midge swarms [Reynolds et al. 2017, Reynolds 2018a,b, van der Vaart et al. 2019]. I show that tensile strength can be attributed to the presence of centre-of-mass movements (i.e., to heat), as documented by Reynolds and Ouellette [2016]. This new result along with earlier results [Reynolds et al. 2017,
50 Reynolds 2018a,b, van der Vaart et al. 2019] shows how the suite of observed complex, emergent, macroscopic behaviours of insect swarms [Kelley and Ouellette 2013, Ni and Ouellette 2016, Sinhuber and Ouellette 2017, Sinhuber et al. 2019, Kasper et al. 2019] can be attributed to simple processes and encapsulated within a simple model [Reynolds et al. 2017, Reynolds 2018a,b]. This is significant because the development of accurate, generally-
55 applicable models is of central importance, as a check on our understanding of the processes at work within swarms.

The emergence of tensile strength

In the 1-dimensional form of the model of Reynolds et al. [2017] the positions, x , and velocities, u , of insects within a swarm are determined by the stochastic differential equations

$$\begin{aligned} du &= -\frac{u}{T} dt + \frac{\sigma_u^2}{\rho} \frac{\partial \rho}{\partial x} dt + \sqrt{2B_0} dW_0(t) \\ dx &= u dt \end{aligned} \tag{1}$$

where T is the velocity autocorrelation timescale, σ_u^2 is the velocity variance, $\rho(x)$ is the observed swarm density profile, B_0 is a constant, and $dW_0(t)$ is an incremental Wiener process with correlation property $\overline{dW_0(t)dW_0(t+\tau)} = \delta(\tau)dt$. The first term on the right-hand side of Eqn. (1) is a memory term that causes velocity fluctuations to relax back to their (zero) mean value. Interactions between the individuals are not explicitly modeled; rather, their net effect is subsumed in a restoring force term, since observations have suggested that to leading order insects appear to be tightly bound to the swarm itself but weakly coupled to each other inside it [Kelley and Ouellette 2013]. This restoring force is given by the second term on the right-hand side of Eqn. (1) which ensures that the spatial distribution of the simulated insects matches observations. The third term, the noise term, represents fluctuations in the resultant internal force that arise partly because of the limited number of individuals in the grouping and partly because of the nonuniformity in their spatial distribution. The model, Eqn. 1, is effectively a first-order autoregressive stochastic process in which position and velocity are assumed to be jointly Markovian. At second-order, position, velocity and acceleration would be modelled collectively as a Markovian process. The first order model, Eqn. 1, is appropriate because the acceleration autocorrelation timescale is shorter than the velocity autocorrelation timescale [Reynolds and Ouellette 2016]. By construction, simulated trajectories have homogeneous (position-independent) Gaussian velocity statistics. When the density profile is Gaussian, as it nearly is for laboratory swarms [Kelley and Ouellette 2013], Eqn. 1 reduces to Okubo's [1986] classic model for the simulation of insect trajectories. Similar models have also been used to model robotic swarms [Hamann and Wörn 2008].

In the presence of two swarm makers, swarms are bi-modal and could, for example, be characterised by

$$\rho(x) = \exp\left(\frac{a}{2}x^2 - \frac{b}{4}x^4\right) \quad (2)$$

which has maxima at $x = \pm\sqrt{a/b}$. For such swarms the mean restoring force term

$$-\frac{\sigma_u^2}{\rho} \frac{\partial \rho}{\partial x} = -\sigma_u^2 (ax - bx^3). \text{ The locations of the swarm centres do, however, fluctuate over}$$

90 time [Ouellette and Reynolds 2016]. These fluctuations can be regarded as being ‘parametric’ noise which operationally equates to $a \rightarrow a + \sqrt{2}a_1 dW_1(t)$. In this case the model becomes

$$\begin{aligned} du &= -\frac{u}{T} dt + \frac{\sigma_u^2}{\rho} \frac{\partial \rho}{\partial x} dt + \sqrt{2B_0} dW_0(t) + \sqrt{2B_1} x dW_1 \\ dx &= u dt \end{aligned} \quad (3)$$

This new model corresponds to the Fokker-Planck equation

$$\frac{\partial p}{\partial t} + u \frac{\partial p}{\partial x} = \frac{\partial}{\partial u} \left(\frac{u}{T} - \frac{\sigma_u^2}{\rho} \frac{\partial \rho}{\partial x} \right) p + (B_0 + B_1 x^2) \frac{\partial^2 p}{\partial u^2} \quad (4)$$

95 where $p(u, x, t)$ is the joint distribution of velocity and position. Here Eqn. 4 is examined in the long-time limit as $t/T \rightarrow \infty$. Here this is done following the approach of Thomson [1987] who identified the conditions under which stochastic models of tracer-particle trajectories in turbulent flows reduce to diffusion-equation models as the Lagrangian velocity-autocorrelation timescale tends to zero. In this approach the unit of time is chosen so that T is small compared

100 with unity and the unit of length is chosen so that the size of a swarm of individuals from a point source is of order unity at times of order unity. In this system of units, velocities must be large to make up for the small timescale. Moreover, because velocities are large and rapidly changing, B_0 and B_1 must also be large. Simple scaling arguments indicate that the long-time

limit of Eqn.4 can be examined by replacing T, u, B_0 and B_1 with $\varepsilon^2 T, \varepsilon^{-1} u, \varepsilon^{-4} B_0$ and $\varepsilon^{-4} B_1$

105 where $\varepsilon \rightarrow 0$ so that Eqn. 4 becomes

$$\frac{\partial p}{\partial t} + \frac{u}{\varepsilon} \frac{\partial p}{\partial x} = \frac{\partial}{\partial u} \left(\frac{u}{\varepsilon^2 T} - \frac{\sigma_u^2}{\varepsilon \rho} \frac{\partial \rho}{\partial x} \right) p + \frac{1}{\varepsilon^2} (B_0 + B_1 x^2) \frac{\partial^2 p}{\partial u^2} \quad (5)$$

If a different rescaling is adopted, then it can be shown that the dispersal is not of order unity at times of order unity. Following Thomson [1987] I now look for solutions to Eqn. 5 that take the form $p = p_0 + \varepsilon p_1 + \varepsilon^2 p_2 + \dots$

110 The leading order (ε^{-2}) terms give

$$\frac{u}{T} p_0 + (B_0 + B_1 x^2) \frac{\partial p_0}{\partial u} = 0, \text{ i.e., } p_0 = \frac{c(x,t)}{\sqrt{B_0 + B_1 x^2}} \exp\left(-\frac{u^2}{2(B_0 + B_1 x^2)T}\right) \quad (6)$$

where $c(x,t)$ is the swarm density profile predicted by the new model, Eqn. 4.

At order ε^{-1}

$$u \frac{\partial p_0}{\partial x} - \frac{\sigma_u^2}{B_0 + B_1 x^2} \frac{u}{T\rho} \frac{\partial \rho}{\partial x} p_0 = \frac{\partial}{\partial u} \left(\frac{u}{T} p_1 + (B_0 + B_1 x^2) \frac{\partial p_1}{\partial x} \right) \quad (7)$$

115 At order ε^0

$$\frac{\partial p_0}{\partial t} + u \frac{\partial p_1}{\partial x} = \frac{\partial}{\partial u} \left(\frac{u}{T} - \frac{\sigma_u^2}{\rho} \frac{\partial \rho}{\partial x} \right) p_2 + (B_0 + B_1 x^2) \frac{\partial^2 p_2}{\partial u^2} \quad (8)$$

which after integrating over all velocities becomes

$$\frac{\partial c}{\partial t} + \frac{\partial}{\partial x} \int u p_1 du \left(\frac{\partial c}{\partial x} - \frac{1}{B_0 + B_1 x^2} \left(B_1 x^2 + \frac{c}{\rho} \frac{\partial \rho}{\partial x} \right) \right) = 0 \quad (9)$$

i.e., becomes the non-linear diffusion equation

$$120 \quad \frac{\partial c}{\partial t} = K \frac{\partial}{\partial x} \left(\frac{\partial c}{\partial x} - \frac{B_0}{B_0 + B_1 x^2} \left(B_1 x^2 + \frac{c}{\rho} \frac{\partial \rho}{\partial x} \right) \right) \quad (10)$$

where from Eqn. 7, p_1 is the solution to

$$\frac{u}{\sqrt{B_0 + B_1 x^2}} \exp\left(-\frac{u^2}{2T(B_0 + B_1 x^2)}\right) = \frac{\partial}{\partial u} \left(\frac{u}{T} p_1 + (B_0 + B_1 x^2) \frac{\partial p_1}{\partial x} \right) \quad (11)$$

and where $K = -\int u p_1 du$. Hence the non-linear Langevin equation, Eqn. 3, reduces to a diffusion equation in the limit $t/T \rightarrow \infty$. The density profiles are determined by Eqn. 9 those

125 steady-state solution is

$$c(x) = \frac{N}{\sqrt{B_0 + B_1 x^2}} \exp\left(\frac{B_0 (aB_1 + bB_0) \ln(B_0 + B_1 x^2) - bB_0 B_1 x^2}{2B_1^2}\right) \quad (12)$$

where N is normalization constant. This theoretical prediction is supported by the results of numerical simulations using the non-linear Langevin equation, Eqn. 3 (Fig. 1). A directly

130 analogous result was obtained by Okubo [1986], albeit in a different context and for diffusion models rather than for non-linear Langevin equation, Eqn. 3.

In the absence of parametric noise, Eqn. 12 rightly reduces to the unperturbed density profile, $\rho(x)$ (Eqn.2). When the parametric noise, B_1 , is small, Eqn.12 has maxima close to the maxima of $\rho(x)$ but displaced towards the origin (Fig. 1). And when the relative strength of
135 the parametric noise $B_1 / B_0 > a$ there this a single maximum at the origin that becomes more pronounced as B_1 / B_0 increases (Fig. 1). The swarm therefore appears to be in tension with a tensile strength that increases with increasing B_1 / B_0 . Similarly as a pair of swarm markers are pulled apart, two daughter swarms form that are effectively pulled away from their respective markers and into the neck that links them, mirroring the observations of Ni
140 and Ouellette [2016] (Fig. 2). This demonstrates that the simulated swarms, like real swarms, possess an emergent analogue of a finite Young's modulus and do not show a viscous flow regime; if they did then they would be expected to either flow back into a single swarm or to form two completely distinct swarms centred over their respective markers [Ni and Ouellette 2016]. Moreover, when the marker separation becomes large enough, the model predicts that
145 the two daughter swarms become fully distinct and that individuals no longer pass between them (Fig. 2). The simulated swarms like the real swarms [Ni and Ouellette 2016] therefore possess yield strengths.

The results of numerical simulations (not shown) suggest that the emergence of tensile
150 strength is a general consequence of parametric noise, arising for example when the 4th-order term rather than the 2nd-order term in the unperturbed density profile, Eqn.2, is noisy.

Discussion

155 Male midges swarm to provide a mating target for females, making stationarity desirable. Ni and Ouellette [2016] were the first to show that this biological function is reflected in an emergent physical macroscopic property of the swarm; namely its tensile strength. This emergent macroscopic mechanical property may be advantageous, in helping to stabilise insect swarms against environmental perturbations. Perturbations are inevitable in wild (natural) swarms that must contend with gusts of wind and with environmental disturbances.

160 Here it was shown that the tensile strength of swarms can (somewhat counter-intuitively) to be attributed to centre-of-mass movements, as documented by Reynolds and Ouellette [2016] (Figs. 1 and 2). This may explain *how* these swarms possess enhanced properties relative to individual insects.

165 As the swarm size increases, centre-of-mass movements are determined by a balance between two competing effects: namely averaging over more but larger fluctuations because insects behave as if they are more weakly bound when in larger swarms [Kelley and Ouellette 2013]. The results of preliminary numerical simulations (not shown) suggest that the latter outweighs the former and that consequently centre-of-mass movements and so tensile
170 strength increases with increasing swarm size. Insect swarms are therefore predicted to 'solidify' as they increase in size, making it harder to pull them apart. This new prediction could be tested in the laboratory by measuring tensile strength as a function of swarm size. If true, then it suggests that insect swarms effectively cool as they increase in size. Fire ants, on the other hand, which link their bodies to form dense aggregations, behave more like viscoelastic
175 fluids, becoming stiffer and more purely elastic as the density of the ants increases [Tennenbaum et al. 2016, Vernerey et al. 2018]. Active changes in group morphology in response to dynamic loads are also evident in dense tree-hanging clusters of honeybees [Peleg et al. 2018].

180 The identification and understanding of the emergent macroscopic properties of insect swarms holds promise of a unified 'thermodynamic' theory of insect swarms, where one seeks to describe their mechanical-like properties in a way that does not directly reference individual behaviours [Ouellette 2017]. In such a theory different swarm morphologies and dynamics might be regarded as being different phases of insect swarming behaviour. This notion may
185 help reconcile conflicting observations of insect swarms made in quiescent laboratory conditions and in the wild [Kelley and Ouellette 2013, Attanasi et al. 2014] because, as was shown here and as was prefigured in Reynolds (2018b), perturbations may drive phase transitions.

190

Acknowledgements

The work at Rothamsted forms part of the Smart Crop Protection (SCP) strategic programme (BBS/OS/CP/000001) funded through the Biotechnology and Biological Sciences Research Council's Industrial Strategy Challenge Fund. I thank Nick Ouellette, Michael Sinhuber and Kasper van der Vaart for encouraging communications.

References

Attanasi, A., Cavagna, A. et al. Collective behaviour without collective order in wild swarms of midges. *PLoS Comp. Biol.* **10**, e1003697 (2014).

Hamann, H. & Wörn, H. A framework of space-time continuous models for algorithm design of swarm robotics. *Swarm Intell.* **2**, 209-239 (2008).

Kelley, D.H. & Ouellette, N.T. Emergent dynamics of laboratory insect swarms. *Sci. Rep.* **3**, 1073, 1-7 (2013).

Ni, R. & Ouellette, N.T. On the tensile strength of insect swarms. *Phys. Biol.* **13**, 045002 (2016).

Okubo, A. Dynamical aspects of animal grouping: swarms, schools, flocks and herds. *Adv. Biophys.* **22**, 1-94 (1986).

Ouellette, N.T. Toward a "thermodynamics" of collective behavior, *SIAM News* **50**, (2017).

Peleg, O., Peters, J.M., Salcedo, M.K. & Mahadevan, L. Collective mechanical adaptation of honeybee swarms. *Nat. Phys.* **14**, 1193-1198 (2018).

Puckett, J.G., Kelley, D.H. & Ouellette, N.T. Searching for effective forces in laboratory insect swarms. *Sci. Rep.* **4**, 4766 (2014).

Reynolds A.M. & Ouellette N.T. Swarm dynamics may give rise to Lévy flights. *Sci. Rep.* **6**, 30515 (2016).

225 Reynolds, A.M., Sinhuber M. & Ouellette N.T. Are midge swarms bound together by an effective velocity-dependent gravity? *Euro. Phys. J. E* **40**,46 (2017).

Reynolds, A.M. Langevin dynamics encapsulate the microscopic and emergent macroscopic properties of midge swarms. *J. Roy. Soc. Inter.* **15**, 20170806 (2018a).

230

Reynolds, A.M. Fluctuating environments drive insect swarms into a new state that is robust to perturbations. *Europhys. Lett.* **124**, 38001, (2018b).

235 Sinhuber, M. & Ouellette, N.T. Phase coexistence in insect swarms. *Phys. Rev. Lett.* **119**, 178003 (2017).

Sinhuber, M., van der Vaart, K. & Ouellette, N.T. Response of insect swarms to dynamic illumination perturbations. *J. R. Soc. Interface* 20180739 (2019).

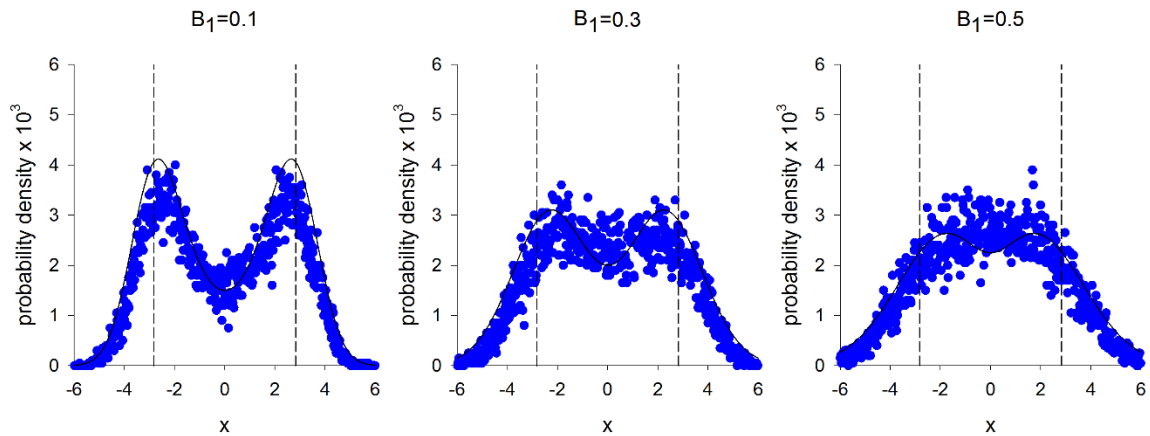
240 Tennenbaum, M., Liu, Z., Hu, D. & Fernandez-Nieves, A. Mechanics of fire ant aggregations. *Nat. Mat.* **15**, 54-59 (2016).

Thomson, D.J. Criteria for the selection of stochastic models of particle trajectories in turbulent flows. *J. Fluid Mech.* **180**, 529-556 (1987).

245

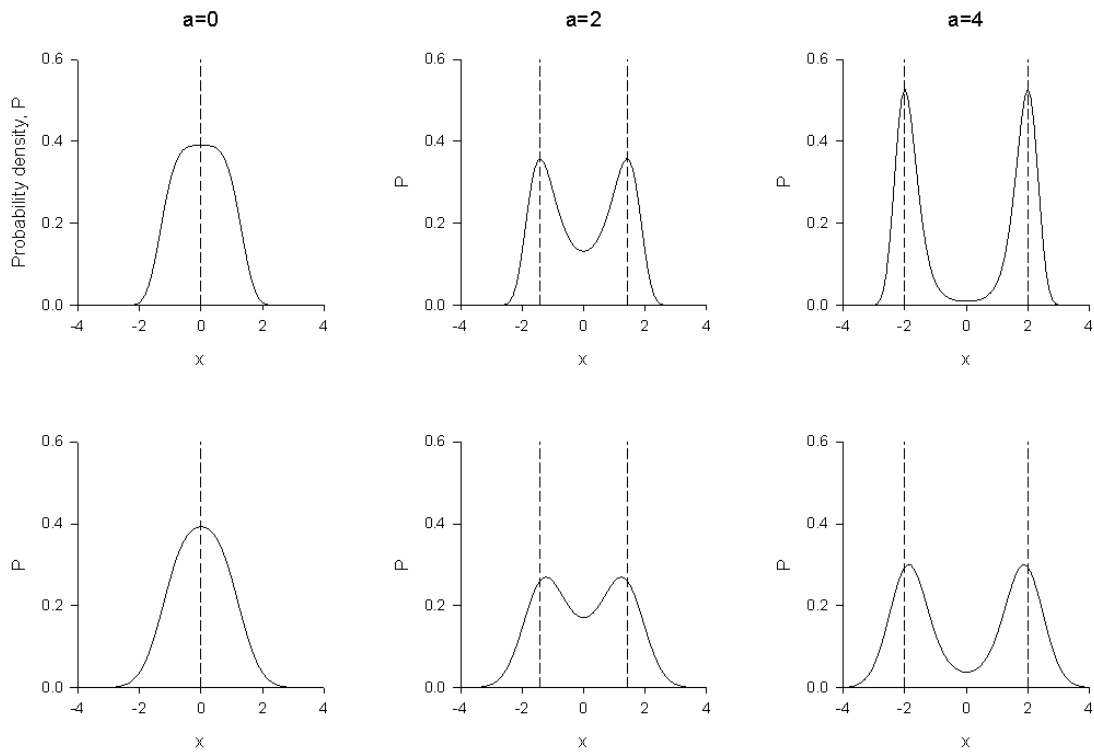
Vaart, van der K., Sinhuber, M., Reynolds, A.M. & Ouellette, N.T. Mechanical spectroscopy of insect swarms (Submitted) (2019).

250 Vernerey, F.J., Shen, T., Sridhar, S.L. & Wagner, R.J. How do fire ants control the rheology of their aggregations. *J. Roy. Soc. Int.*, **15**, 20180642 (2018).



255

Figure 1. Theoretical predictions for swarm density profiles match data from numerical simulations. The swarms are being pulled away from their respective swarm markers (dashed-lines) and displaced towards the origin. The swarms therefore appear in tension with a tensile strength that increases as centre-of-mass movements increase. Predictions (solid line) obtained from Eqn. 12 are shown for $a=0.8$, $b=0.1$ and $B_0=1$ with $B_1=0.1$ (left), 0.3 (middle) and 0.5 (right). Simulation data (\bullet) were obtained from Eqn. 3 for $\sigma_u^2=1$ and $T=1$.



265 **Figure 2. In the presence of parametric noise insect swarms are predicted to have an emergent analogue of a finite Young's modulus and yield stress, and do not show a viscous flow regime.** When parametric noise is absent ($B_1=0$) the swarm is always localized over the swarm markers ($x = \pm\sqrt{a/b}$) (dashed lines) as it is pulled apart and so not in tension (upper panel). When parametric noise is present ($B_1=1.0$) the swarm is put into tension as it is pulled apart as the swarms are being pulled away from their respective swarm markers (dashed-lines) and displaced towards the origin (lower panel) This displacement decreases with increasing separation of the swarm markers. Predictions obtained from Eqn. 12 are shown for $a=0$ (left), 2 (middle) and 4 (right), and $b=0.25$.

270